

# Modeling of bare and aspirated thermocouples in compartment fires

Linda G. Blevins\*, William M. Pitts

*Building and Fire Research Laboratory, National Institute of Standards and Technology, 100 Bureau Drive,  
Stop 8653, Gaithersburg, MD 20899-8653, USA*

Received 29 March 1999; received in revised form 26 July 1999; accepted 27 July 1999

## Abstract

As part of an effort to characterize the uncertainties associated with temperature measurements in fire environments, models of bare bead, single-shielded aspirated, and double-shielded aspirated thermocouples were developed and used to study the effects of varying the gas and average effective surroundings temperatures on the thermocouple error of each configuration. The models were developed for steady-state conditions and hence provide information about error trends rather than about absolute error values. The models indicate that thermocouples respond differently to changes in effective surroundings temperature in a hot upper-layer than in a relatively cooler lower layer of a room fire. In an upper-layer, for a given gas temperature, the thermocouple error is relatively insensitive to surroundings temperature. In a lower layer, errors which increase rapidly with surroundings temperature are possible. The most extreme errors occur in a lower layer when the gas temperature is low and the surroundings temperature is high. Aspirated thermocouples reduce the errors in both the upper and lower layers of a room fire, but do not eliminate them entirely. The present study is intended to provide fire researchers with a methodology for developing working models of thermocouples which are tailored to their own configurations. Published by Elsevier Science Ltd.

## 1. Introduction

Measuring gas temperature in and around fires is important for verifying and validating computer models and for gaining an empirical understanding of complex fire behavior. The most common way to measure temperature during fire testing is to

---

\* Corresponding author. Tel.: + 001-301-975-3904; fax: + 001-301-975-4052.  
E-mail address: [linda.blevins@nist.gov](mailto:linda.blevins@nist.gov) (L.G. Blevins)

### Nomenclature

$A_j, A_k$	surface area of arbitrary surface $j$ or $k$ , $m^2$
$A_b$	surface area of thermocouple bead, $m^2$
$A_c$	annular flow area of double-shielded probe, $m^2$
$A_i$	surface area of the innermost shield for double-shielded probe, $m^2$
$A_o$	surface area of outermost shield for single- and double-shielded probes, $m^2$
$C_{i \rightarrow o}$	geometric constant defined for double-shielded model
$D_{char}$	characteristic length used for defining Nusselt number, m
$D_b$	thermocouple bead diameter, m
$D_h$	hydraulic diameter of annular region of double-shielded probe, m
$D_i$	innermost shield diameter for double-shielded probe, m
$D_o$	outermost shield diameter for single- and double-shielded probes, m
$F_{jk}$	radiation configuration factor between surfaces $j$ and $k$
$h_{bU}$	convective heat transfer coefficient between external gas flow and bare thermocouple bead, $W/m^2 K$
$h_{bu}$	convective heat transfer coefficient between aspirating gas flow and thermocouple bead for single- and double-shielded probes, $W/m^2 K$
$h_{iu}$	convective heat transfer coefficient between aspirating gas flow and innermost shield for double-shielded probe, $W/m^2 K$
$h_{iw}$	convective heat transfer coefficient between annular aspirating gas flow and innermost shield for double-shielded probe, $W/m^2 K$
$h_{jv}$	convective heat transfer coefficient between gas with velocity $v$ and arbitrary surface $j$ , $W/m^2 K$
$h_{ou}$	convective heat transfer coefficient between aspirating gas flow and shield for single-shielded probe, $W/m^2 K$
$h_{oU}$	convective heat transfer coefficient between external gas flow and outermost shield for single- and double-shielded probes, $W/m^2 K$
$h_{ow}$	convective heat transfer coefficient between annular aspirating gas flow and outermost shield for double-shielded probe, $W/m^2 K$
$k_g$	gas thermal conductivity, $W/mK$
$L$	distance from probe inlet to thermocouple bead for single- and double-shielded probes, m
$Nu_{jv}$	Nusselt number for gas with velocity $v$ and arbitrary surface $j$
$P_w$	wetted perimeter of annulus for double-shielded probe, m
$q_{rad j \rightarrow k}$	rate of radiative heat transfer from surface $j$ to surface $k$ , W
$q_{conv j, v}$	rate of convective heat transfer from a gas with velocity $v$ to surface $j$ , W
$T_b$	thermocouple bead temperature, $^{\circ}C$ or $K$
$T_g$	gas temperature, $^{\circ}C$ or $K$
$T_i$	innermost shield temperature for double-shielded probe, $^{\circ}C$ or $K$
$T_j, T_k$	temperature of arbitrary surface $j$ or $k$ , $^{\circ}C$ or $K$

$T_o$	outermost shield temperature for single- and double-shielded probes, °C or K
$T_\infty$	average effective surroundings temperature, °C or K
$u$	aspiration velocity across thermocouple bead for single- and double-shielded probes, m/s
$U$	external fire-induced flow velocity, m/s
$w$	aspiration velocity in the annulus for double-shielded probe, m/s
$\Delta T$	thermocouple error, absolute value of the difference between $T_g$ and $T_b$ , °C or K
$\varepsilon_b$	thermocouple bead emissivity
$\varepsilon_o$	outermost shield emissivity for single- and double-shielded probes
$\varepsilon_i$	innermost shield emissivity for double-shielded probe
$\varepsilon_j, \varepsilon_k$	emissivity of arbitrary surface $j$ or $k$
$\sigma$	Stefan-Boltzmann constant, $5.67 \times 10^{-8} \text{ W/m}^2 \text{ K}^4$

use bare thermocouples. However, the temperature indicated by a bare thermocouple near an enclosure fire differs from the true gas temperature because the bead exchanges radiation with the room walls, the hot flame gases and soot, and the ambient environment through doors and windows. Radiation corrections are difficult to perform during fire testing for several reasons. First, selecting an effective surroundings temperature is arduous because of the temporally and spatially varying environment. In addition, the local convection velocity and gas composition vary and are not usually known. The emissivity of the thermocouple bead varies with temperature and with exposure to fire environments; soot can accumulate, changing the bead diameter and its thermophysical properties. Finally, convective heat transfer correlations are based on experiments and have high uncertainties [1]. Because of these difficulties, fire researchers often perform experiments without considering radiation losses or gains on thermocouples. Unfortunately, this procedure can yield ambiguous gas temperature readings [2,3]. NIST is presently working to characterize experimentally these ambiguities [4,5]. The present paper describes idealized heat transfer modeling of thermocouples in fire environments performed in support of the NIST effort.

One way to reduce the effect of external radiative exchange on a thermocouple measurement is to use an aspirated thermocouple, which consists of a thermocouple enclosed in one or more cylindrical radiation shields. The gas to be measured is pulled axially through the shield(s) using a pump or other aspiration device. The shield(s) reduce the radiative exchange between the thermocouple and its surroundings, while the rapid flow increases the convective exchange between the gas and the thermocouple. The result is that the temperature indicated by an aspirated thermocouple is closer to the true gas temperature than that indicated by a bare thermocouple of similar bead size.

While using an aspirated thermocouple favorably reduces the influence of radiation on the measurement, temporal and spatial resolution are sacrificed. In addition,

aspirated thermocouples are cumbersome. For example, during a recent NIST study, a large ice bath, two dry ice traps, and two glass wool filters were necessary in each aspirated thermocouple sampling line to protect the vacuum pump and rotameter from water damage and soot clogging [5]. This is especially constraining when many thermocouples are used simultaneously, which is generally desirable for fire studies. Because aspirated thermocouples involve tradeoffs in resolution and ease of use, the individual researcher must decide if the improvements offered by their use justify the extra effort to use them.

The goal of the present research was to use idealized modeling to elucidate the ways that bare and aspirated thermocouples respond to the thermal environments present in fires. The behaviors of thermocouples exposed to conditions characteristic of upper and lower layers of a room fire were predicted. The modeling was performed to help researchers (1) make informed thermocouple choices when planning experiments, and (2) understand the uncertainties in thermocouple measurements while and after they are made.

Several papers have been published on the design and use of aspirated thermocouples, also known as “suction pyrometers”, in furnaces, gas turbines, and other combustion environments [6–23]. These works generally emphasize applications where (1) the temperature of the surrounding walls is lower than the temperature of the gas, and (2) the gas and surroundings temperature do not differ appreciably (but are large enough to warrant concern). In a room fire, which often consists of a relatively cool lower gas layer and a generally hot upper gas layer, these two conditions are not always satisfied. Hence, examination of aspirated thermocouples in *fire* environments is warranted. To the authors’ knowledge, Newman and Croce published the only study focusing on the design of aspirated thermocouples for fire research [24]. They developed a prototype aspirated thermocouple which featured a 1.8-mm-diameter thermocouple bead enclosed in a 6.4-mm-diameter steel shield. Newman and Croce tested their instrument by increasing the flow through the probe until the measured temperature approached a value which seemed independent of aspiration velocity. Based on this technique, they concluded that an aspiration velocity of about 7 m/s was adequate to obtain a temperature “which should correspond to the true gas temperature [24]”. The American Society for Testing and Materials (ASTM), in the *Standard Guide for Room Fire Experiments*, similarly recommends that the aspiration velocity be maintained near 5 m/s, stating that this is “sufficiently high to allow accurate temperature measurement based on thermocouple voltage alone, even within flame zones [25]”. Luo, in a recent paper addressing radiation effects on thermocouples in fires, stated that the use of an aspirated thermocouple with a 2-m/s aspiration velocity “gives the true gas temperature [3]”. In contrast, previously published studies of aspirated thermocouples recommend aspiration velocities between 100 and 300 m/s (e.g. Refs. [6,7,10,16]). This contradiction in recommended aspiration velocity is addressed during the present work.

Heat transfer models for bare-bead, single-shielded aspirated, and double-shielded aspirated thermocouples are described in this paper. Modeling results are used to (1) demonstrate that thermocouples behave differently in the upper and lower layers

of a room fire, (2) establish the potential for aspirated thermocouples to reduce errors in room fire temperature measurements, and (3) illustrate that the ASTM-recommended 5-m/s aspiration velocity is not always fast enough to obtain accurate measurements around fires.

## 2. Model development

The bare-bead, single-shielded aspirated, and double-shielded aspirated thermocouple models were developed using steady-state, combined-mode heat transfer analysis with graybody-enclosure radiative exchange [26]. Important model development details are summarized here. Full derivations of the equations are given elsewhere [5]. The graybody enclosure analysis involves assuming that all surfaces are isothermal and opaque, and that they possess absorptivities and emissivities which are independent of wavelength and temperature. It also involves assuming that all emitted, reflected, and incident radiation has the same intensity in all directions. Arguments for the appropriateness of the graybody enclosure analysis are available [27].

For the purpose of capturing the basic physics of a thermocouple responding to its environment, it is assumed that heat is added to or removed from the surroundings in an unspecified amount which allows them to remain at a constant effective temperature,  $T_{\infty}$ . The surroundings temperature  $T_{\infty}$  represents the effective radiation temperature of the potentially multi-temperature surrounding environment. It does not represent the temperature of any single object in a room; rather, it can be thought of as the temperature of an imaginary enclosure which would exchange radiation with the thermocouple at a rate equivalent to the net radiative exchange rate experienced by the thermocouple in its multi-object environment.

All gases are assumed to be isothermal for the present analysis. Neglecting temperature gradients in gases and on surfaces should not affect the general behavioral trends presented in this paper; including them would immensely complicate the formulation. The thermophysical properties of the gases are assumed to be those of air, calculated using polynomial curve fits of tabulated values [28]. This is reasonable since air (composed mostly of nitrogen) is a constituent of most fire gases. Consistent with previous experimental findings [29], a fire-induced gas flow, with a velocity of  $U$ , is assumed to exist in the vicinity of the thermocouple. Gases are assumed to be radiatively non-participating, which is valid for small optical depths. For large optical depths, hot gas and/or soot may partially or fully attenuate radiative exchange between a thermocouple and its surroundings; hence, if a thermocouple is immersed in an optically thick region (such as in the upper-layer of a sooty fire), the present models do not apply [4,5]. For the aspirated thermocouple models, radiative exchange between the thermocouple bead and its local surroundings through its shield opening is neglected. This assumption is valid *only* if the shield opening faces a region with a temperature similar to the shield temperature. In reality, radiative exchange through the opening during a fire can alter the effectiveness of an aspirated thermocouple [4,5]. While the magnitude of the predicted errors will be affected by this type of exchange, the behavioral trends predicted here should not.

All radiation interchange is modeled as two-body exchange (i.e., each surface ‘sees’ only one other surface). Hence, the radiative heat transfer between surfaces  $j$  and  $k$  is written as [28]

$$q_{rad\ j \rightarrow k} = \frac{(\sigma T_j^4 - \sigma T_k^4)}{(1 - \varepsilon_j)/\varepsilon_j A_j + 1/F_{jk} A_j + (1 - \varepsilon_k)/\varepsilon_k A_k}, \quad (1)$$

where  $F_{jk}$  is the fraction of radiant energy leaving surface  $j$  which strikes surface  $k$ . This equation is valid if surface  $j$  is completely enclosed in surface  $k$ . If surface  $j$  is convex ( $F_{jk} = 1$ ) and has much smaller area than surface  $k$  ( $A_j/A_k \ll 1$ ), then Eq. (1) reduces to

$$q_{rad\ j \rightarrow k} = \varepsilon_j A_j (\sigma T_j^4 - \sigma T_k^4). \quad (2)$$

If surface  $j$  is convex and has an area which is comparable to the area of surface  $k$ , then Eq. (1) reduces to

$$q_{rad\ j \rightarrow k} = \frac{A_j (\sigma T_j^4 - \sigma T_k^4)}{1/\varepsilon_j + (A_j/A_k)(1 - \varepsilon_k)/\varepsilon_k}. \quad (3)$$

All convective heat transfer is modeled using Newton’s law of cooling, which for convection from a gas with a velocity  $v$  to a surface  $j$  is written as [28]

$$q_{conv\ j,v} = h_{jv} A_j (T_g - T_j). \quad (4)$$

The convective heat transfer coefficients are calculated using correlations developed for the Nusselt number, defined for surface  $j$  and gas velocity  $v$  as [28]

$$Nu_{jv} = \frac{h_{jv} D_{char}}{k_g}. \quad (5)$$

The characteristic length,  $D_{char}$ , is defined based on the geometry of interest. The conductivity,  $k_g$ , is evaluated either at  $T_g$  or at the average of the gas and solid temperatures, depending on the convention defined when the correlation of interest was developed [1,28].

The governing equations were kept in dimensional form for the present study. While nondimensionalization minimizes the number of parameters to be varied when analyzing a problem, it proves to be difficult when equations have both fourth- and first-order terms, and when heat transfer correlations depend on local conditions in a complex way. Keeping the model equations in dimensional form allows the present study to be focused on regions of room fires (upper and lower layers) which are physically identifiable using reasonable values of the gas and surroundings temperatures.

The thermocouple error,  $\Delta T$ , used to evaluate a particular thermocouple’s effectiveness, is defined as the absolute value of the difference between the thermocouple bead temperature and the true gas temperature

$$\Delta T = |T_b - T_g|. \quad (6)$$

It is important to note that the absolute magnitudes of the thermocouple errors reported in this paper are strong functions of the particular modeling parameters selected. Hence the reader should focus on the *trends* described rather than on the absolute errors. These trends provide useful general information about the behavior of thermocouples in fire environments, and they provide insight into performance differences between bare bead, single- and double-shielded aspirated configurations in upper and lower layers of room fires.

Probe and bead sizes were selected to closely match those used in recent NIST experiments [4,5]. The baseline parameters were aspiration velocity  $u = 5$  m/s (recommended by ASTM [25]), emissivities  $\varepsilon_b = \varepsilon_o = \varepsilon_i = 0.8$  (typical values for dull, oxidized metal [28]), fire-induced flow velocity  $U = 0.5$  m/s (typically 0–2 m/s in enclosure fires [29]), and bead diameter  $D_b = 1.5$  mm (three times the wire diameter of 0.5 mm used for rigidity in aspirated probes [5,30])<sup>1</sup>. The 1.5-mm bead diameter and 0.5-mm wire diameter were used for all calculations presented here, allowing direct comparison of bare-bead results with aspirated-thermocouple results.

This paper presents two parametric studies. First, solutions for thermocouples exposed to various combinations of  $T_g$  and  $T_\infty$  are given. Second, solutions for a single-shielded aspirated thermocouple operating with various aspiration velocities are presented. Detailed results of a full parametric study are described elsewhere [5].

It should be noted that the modeling presented here does not include transient effects. This is limiting because the temperature indicated by a thermocouple is a complex function of its temporal response behavior, the rate of change of both  $T_g$  and  $T_\infty$ , and the time constants of radiative and convective heat transfer. However, the present steady-state modeling can be used to understand the driving forces behind this transient behavior, and may be used as a building block for future transient characterization efforts. A discussion of experiments designed to examine transient effects appears elsewhere [4,5].

### 2.1. Bare-bead model equations

A schematic (not to scale) of the bare-bead thermocouple is shown in Fig. 1. Heat is transferred to or from the bead via convection and radiation. Radiative exchange between the bead and surroundings can be modeled by Eq. (2). The energy balance on the bead then yields

$$h_{bU}(T_g - T_b) = \varepsilon_b \sigma (T_b^4 - T_\infty^4) \quad (7)$$

or

$$T_b^4 [\varepsilon_b \sigma] + T_b [h_{bU}] - [\varepsilon_b \sigma T_\infty^4 + h_{bU} T_g] = 0. \quad (8)$$

<sup>1</sup> In order to adequately describe the choice of model parameters, it is occasionally necessary to identify commercial products by manufacturer's name or label. In no instance does such identification imply endorsement by the National Institute of Standards and Technology, nor does it imply that the particular products or equipment are necessarily the best available for that purpose.

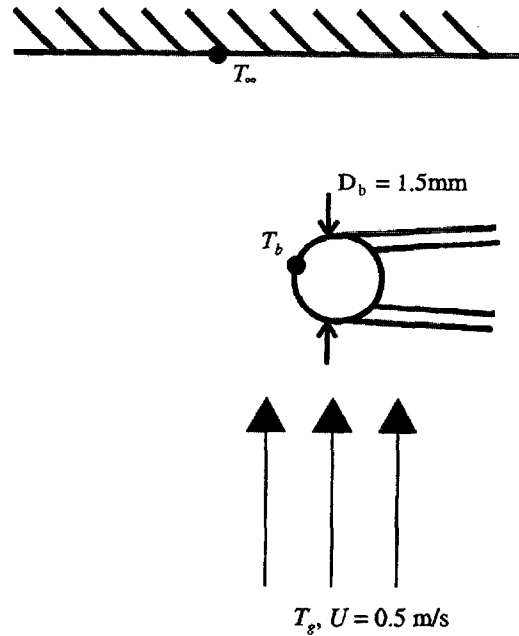


Fig. 1. Schematic of bare thermocouple bead (not to scale). The arrows denoting the external flow velocity,  $U$ , are drawn to show an example of one possible flow direction.

The convective heat transfer coefficient between the external gas flow and the thermocouple bead,  $h_{bU}$ , is estimated using Whitaker's correlation for external flow over a sphere [1]. Calculated Nusselt numbers based on  $D_b$  and  $U$  are accurate to within  $\pm 25\%$  (no coverage factor provided) [1]. For a given gas temperature and surroundings temperature, Eq. (8) is solved for the thermocouple temperature,  $T_b$ , using a first-order Newton's method.

## 2.2. Single-shield model equations

A schematic (not to scale) of the single-shielded aspirated thermocouple is shown in Fig. 2. Convection to the thermocouple bead takes place on its outside surface, while convection to the shield takes place on both its inside and outside surfaces. Radiative exchange between the thermocouple bead and the inner surface of the shield, and between the outer surface of the shield and the surroundings, are modeled using Eq. (2). The energy balances on the bead and shield, respectively, become

$$h_{bu}(T_g - T_b) = \varepsilon_b \sigma (T_b^4 - T_o^4) \quad (9)$$

and

$$h_{ou}(T_g - T_o) + h_{ou}(T_g - T_o) = -\varepsilon_b \sigma \left( \frac{A_b}{A_o} \right) (T_b^4 - T_o^4) + \varepsilon_o \sigma (T_o^4 - T_\infty^4). \quad (10)$$



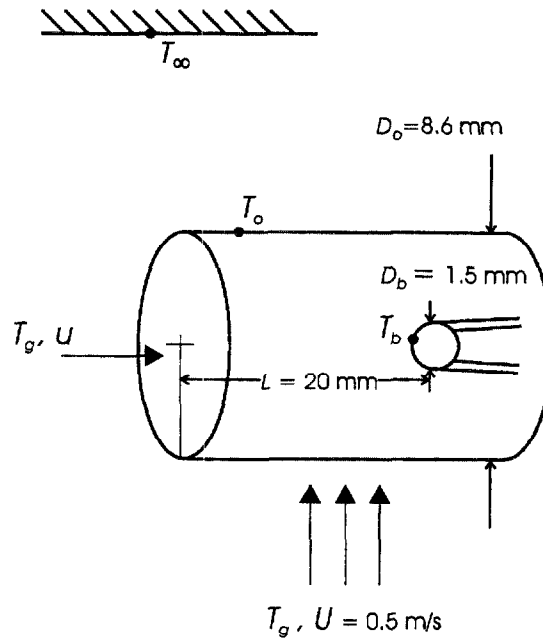


Fig. 2. Schematic of single-shielded aspirated thermocouple (not to scale).

These may be simplified and written in final form as

$$T_b^4[\varepsilon_b\sigma] + T_b[h_{bu}] - [\varepsilon_b\sigma T_o^4 + h_{bu}T_g] = 0 \quad (11)$$

and

$$T_o^4[\varepsilon_o\sigma] + T_o[h_{ou} + h_{ou}] - [\varepsilon_o\sigma T_\infty^4 + (h_{ou} + h_{ou})T_g] = 0. \quad (12)$$

The convective heat transfer coefficient between the aspirating gas flow and the thermocouple bead,  $h_{bu}$ , is estimated using a correlation for a sphere of diameter  $D_b$  with a crossflow velocity equal to the aspiration velocity  $u$ , yielding a Nusselt number accurate within  $\pm 25\%$  (no coverage factor provided) [1]. The convective heat transfer coefficient between the aspirating gas and the shield,  $h_{ou}$ , is computed using a correlation for either developing laminar or fully turbulent flow, with Nusselt numbers based on  $D_o$  and  $u$ . For developing laminar flow, the Seider–Tate correlation for combined entry lengths is used [28]. This correlation is valid for cylinders with uniform wall temperature, yielding Nusselt numbers which are accurate to within  $\pm 25\%$  (no coverage factor provided) [28]. For turbulent flow,  $h_{ou}$  is computed using the correlation developed by Petukhov, Kirillov, and Popov, and modified by Gnielinski [28], with the friction factor defined for smooth tubes. Nusselt numbers calculated using this equation are accurate to within  $\pm 10\%$  (no coverage factor provided) [28]. The correlation for developing flow is applied for very low aspirating velocities, while the turbulent flow correlation is applied for higher velocities (see Ref. [5] for details). The calculated bead temperature is not a strong function of the choice

between these correlations [5]. The convective heat transfer coefficient between the external gas stream and the shield,  $h_{oU}$ , is estimated using the Churchill and Bernstein correlation for a cylinder in crossflow, yielding Nusselt numbers based on  $D_o$  and  $U$  accurate to within  $\pm 25\%$  (no coverage factor provided) [28].

For a given  $T_g$  and  $T_\infty$ , Eq. (12) is solved for  $T_o$  using a first-order Newton's method. Using this result, Eq. (11) is subsequently solved for  $T_b$  in similar fashion. When there is no aspiration, the bead and shield equilibrate at a common temperature.

### 2.3. Double-shield model equations

A schematic (not to scale) of the double-shielded aspirated thermocouple is shown in Fig. 3. The double-shielded probe is identical to the single-shielded probe with an inner shield added. Radiative exchange between the thermocouple bead and the inner surface of the inner shield, and between the outer surface of the outer shield and the surroundings, are modeled using Eq. (2). Because the area of the inner shield is *not* significantly smaller than the area of the outer shield, the rate of radiative exchange between the outer surface of the inner shield and the inner surface of the outer shield is described by Eq. (3). If the constant  $C_{i \rightarrow o}$  is defined such that

$$C_{i \rightarrow o} = \frac{1}{1/\varepsilon_i + (A_i/A_o)(1 - \varepsilon_o)/\varepsilon_o}, \quad (13)$$

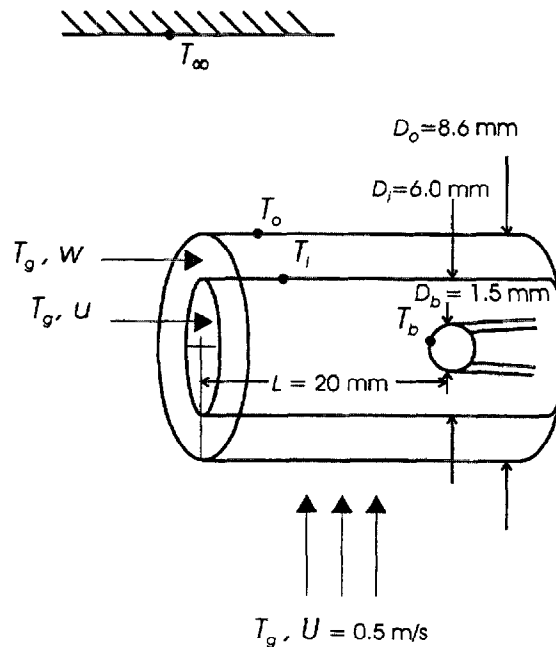


Fig. 3. Schematic of double-shielded aspirated thermocouple (not to scale).

then the energy balances for the bead, inner shield, and outer shield, respectively, become

$$h_{bu}(T_g - T_b) = \varepsilon_b \sigma (T_b^4 - T_i^4), \quad (14)$$

$$h_{iu}(T_g - T_i) + h_{iw}(T_g - T_i) = -\varepsilon_i \sigma \left( \frac{A_b}{A_i} \right) (T_b^4 - T_i^4) + C_{i \rightarrow o} \sigma (T_i^4 - T_o^4) \quad (15)$$

and

$$h_{ow}(T_g - T_o) + h_{ou}(T_g - T_o) = -C_{i \rightarrow o} \sigma \left( \frac{A_i}{A_o} \right) (T_i^4 - T_o^4) + \varepsilon_o \sigma (T_o^4 - T_\infty^4). \quad (16)$$

In final form, these equations are written as

$$T_b^4 [\varepsilon_b \sigma] + T_b [h_{bu}] - [\varepsilon_b \sigma T_i^4 + h_{bu} T_g] = 0, \quad (17)$$

$$T_i^4 [C_{i \rightarrow o} \sigma] + T_i [(h_{iu} + h_{iw})] - [C_{i \rightarrow o} \sigma T_o^4 + (h_{iu} + h_{iw}) T_g] = 0, \quad (18)$$

and

$$T_o^4 [C_{i \rightarrow o} \sigma (A_i/A_o) + \varepsilon_o \sigma] + T_o [(h_{ow} + h_{ou})] - [C_{i \rightarrow o} \sigma (A_i/A_o) T_i^4 + \varepsilon_o \sigma T_\infty^4 + (h_{ow} + h_{ou}) T_g] = 0. \quad (19)$$

The convective heat transfer coefficient between the aspirating gas flow and the thermocouple bead,  $h_{bu}$ , and that between the external gas stream and the outer shield,  $h_{ou}$ , are calculated as for the single-shielded probe. The heat transfer coefficient between the internal gas flow and the inner shield,  $h_{iu}$ , is estimated using the developing and turbulent pipe flow correlations (described previously) based on  $D_i$  and  $u$ . In the annulus,  $h_{iw}$  and  $h_{ow}$  are considered equal, and are calculated using the developing and turbulent pipe flow correlations based on the hydraulic diameter,  $D_h$  [28]. It is customary to define the hydraulic diameter as four times the ratio of the flow area ( $A_c$ ) to the wetted perimeter ( $P_w$ ) [28],

$$D_h = \frac{4A_c}{P_w} = \frac{4(\pi/4)(D_o^2 - D_i^2)}{\pi D_o + \pi D_i} = D_o - D_i. \quad (20)$$

The gas velocity in the annulus ( $w$ ) is assumed to be equal to that through the innermost shield ( $u$ ) for all results reported here.

For a given  $T_g$  and  $T_\infty$ , Eqs. (17)–(19) are solved simultaneously for  $T_b$ ,  $T_i$ , and  $T_o$  using nested Newton's methods. When there is no aspiration, the bead and both shields equilibrate at a common temperature.

### 3. Results and discussion

#### 3.1. Effect of gas and surroundings temperatures

Fig. 4 depicts the absolute value of the temperature error,  $\Delta T$ , predicted for a 1.5-mm bare-bead thermocouple, as a function of  $T_\infty$ , for gas temperatures of 27°C (300 K), 127°C (400 K), 377°C (650 K), 627°C (900 K), and 877°C (1150 K), and 1127°C (1400 K). For these calculations,  $\varepsilon_b = 0.8$  and  $U = 0.5$  m/s. The region where  $T_g$  is higher than  $T_\infty$  is termed the "upper layer", recognizing that the region includes but is not limited to the conditions generally found in the upper layer of a room fire. Similarly, the region where  $T_g$  is lower than  $T_\infty$  is termed the "lower layer". The ovals are printed on the figure to indicate that upper-layer ( $T_g > T_\infty$ ) conditions generally occur on the left side of the graph and lower-layer ( $T_g < T_\infty$ ) conditions occur on the right side. Fig. 4 shows that a bare bead thermocouple behaves differently in the upper and lower layers of a room fire. In the upper layer, the thermocouple indicates a temperature which is lower than that of the gas ( $T_b < T_g$ ). The upper-layer thermocouple error for a given  $T_g$  is relatively insensitive to  $T_\infty$ , decreasing gradually to zero as  $T_\infty$  approaches  $T_g$ . The error is 0°C when  $T_\infty = T_g$ . In the upper-layer

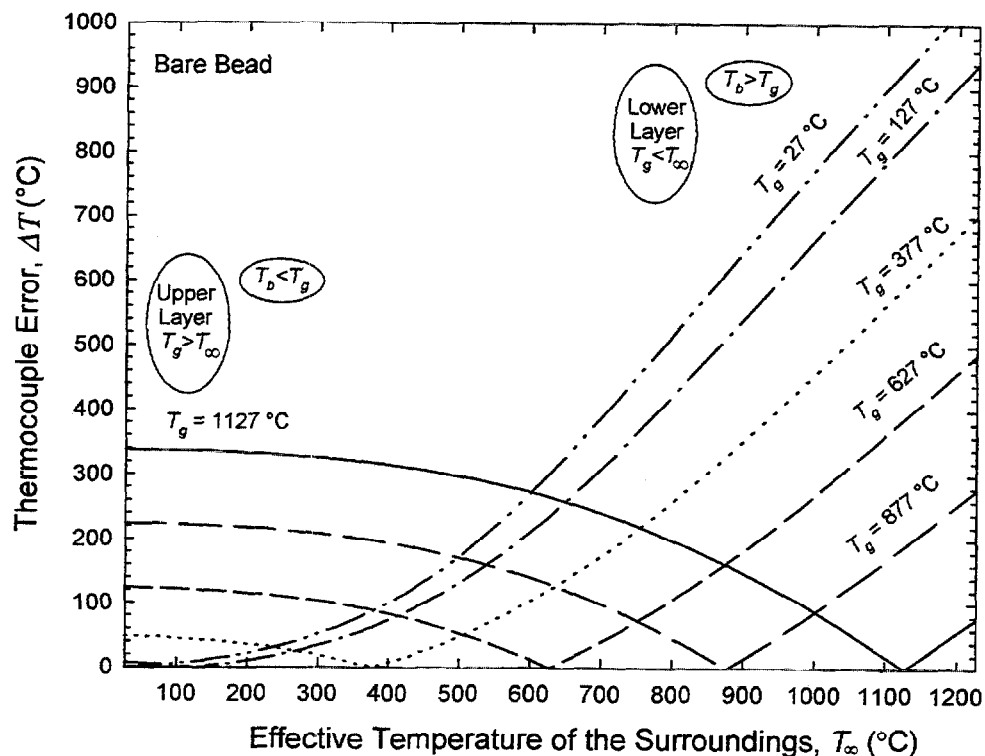


Fig. 4. Effect of surroundings temperature on absolute value of error in measured temperature (from Eq. (6)) for a bare-bead thermocouple with diameter  $D_b = 1.5$  mm, emissivity  $\varepsilon_b = 0.8$ , and external flow velocity  $U = 0.5$  m/s, and gas temperatures of 27°C, 127°C, 377°C, 627°C, 877°C, and 1127°C. The surroundings temperature is that of an imaginary, isothermal enclosure which would exchange radiation with the thermocouple at a rate equivalent to the actual rate it experiences.

region, the thermocouple error increases with increasing  $T_g$ . In contrast, in the lower layer, the thermocouple indicates a temperature which is higher than that of the gas ( $T_b > T_g$ ). The lower layer thermocouple error is a strong function of both  $T_g$  and  $T_\infty$ , increasing more and more rapidly with increasing  $T_\infty$  when the latter value is relatively high. In this region, the thermocouple error decreases with increasing  $T_g$ . The behavior in both regions is controlled by the fourth-order dependence of the radiative heat transfer rate on  $T_\infty$ . The most extreme errors (hundreds of degrees) occur in the lower layer when  $T_g$  is at its lowest assumed value (27°C) and  $T_\infty$  is at its highest (1127°C), which would most likely be encountered only during a fully involved room fire. These modeling results are consistent with experimental findings that errors of greater than 100°C are possible when bare thermocouples are used in fire environments, and that lower-layer errors are more extreme than upper-layer errors [3–5].

Fig. 5 depicts the predicted absolute value of the temperature error for the single-shielded thermocouple. For these calculations,  $u = 5$  m/s,  $\varepsilon_b = \varepsilon_o = 0.8$ ,  $D_b = 1.5$  mm, and  $U = 0.5$  m/s. Fig. 5 demonstrates that the single-shielded probe behaves similarly to the 1.5 mm bare-bead thermocouple, except the errors in the upper and lower layers are reduced for a given  $T_g$  and  $T_\infty$ , and the region of rapidly increasing error in the lower layer is shifted to higher  $T_\infty$ . This shift is expected to decrease the likelihood

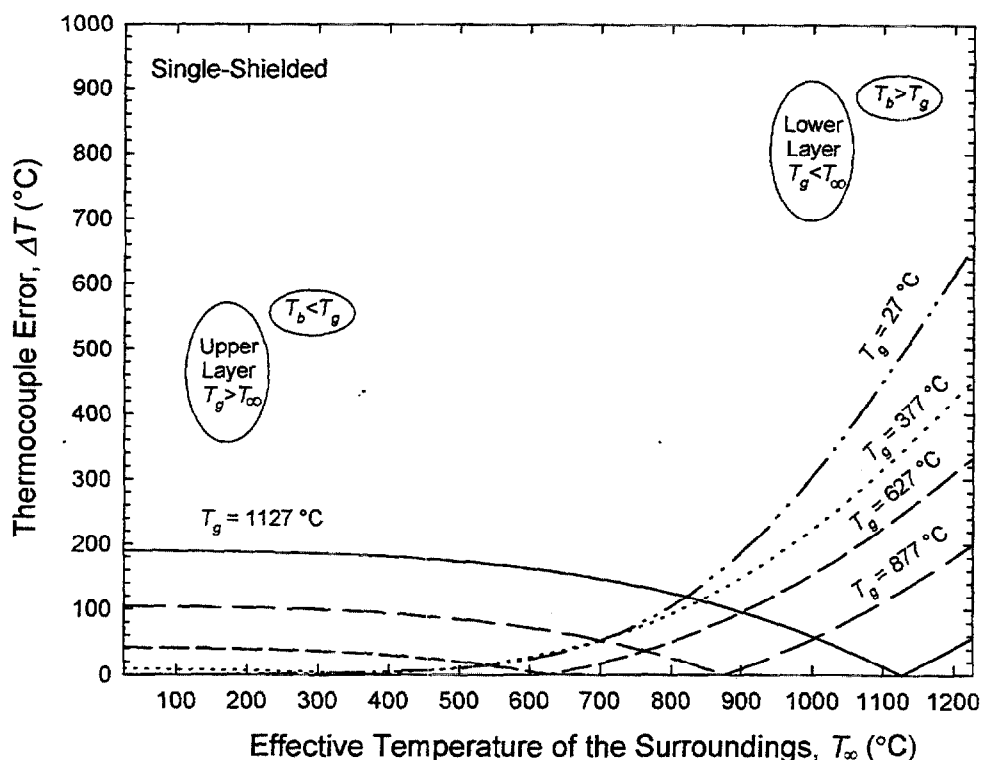


Fig. 5. Effect of surroundings temperature on absolute value of error in measured temperature for a single-shielded aspirated thermocouple, with bead diameter  $D_b = 1.5$  mm, shield diameter  $D_o = 8.6$  mm, emissivities  $\varepsilon_b = \varepsilon_o = 0.8$ , external velocity  $U = 0.5$  m/s, and aspiration velocity  $u = 5$  m/s, and gas temperatures of 27°C, 377°C, 627°C, 877°C, and 1127°C.

that the region of high error will be encountered in an actual room fire test. This conjecture is based on the assumption that the amount of time for which a thermocouple placed in the lower layer will experience a given  $T_\infty$  decreases as  $T_\infty$  increases to  $1100^\circ\text{C}$  and above. The figure shows that the temperature error of the single-shielded thermocouple has an upper bound at about  $190^\circ\text{C}$  for  $T_g = 1127^\circ\text{C}$  in the upper layer, which is about half of the  $340^\circ\text{C}$  upper bound error for the bare-bead thermocouple for the same  $T_g$ . Similar trends occur for the other conditions considered in the figure. Thus, the single shield reduces the steady-state error of the bare-bead thermocouple to about half of its value in the upper layer, and decreases the likelihood that large errors will occur in the lower layer.

Fig. 6 depicts the absolute value of the temperature error for the double-shielded thermocouple. The range of the ordinate axis is half that of the ordinate axes in Figs. 4 and 5. For these calculations,  $u = 5\text{ m/s}$ ,  $w = 5\text{ m/s}$ ,  $\varepsilon_b = \varepsilon_o = \varepsilon_i = 0.8$ ,  $D_b = 1.5\text{ mm}$ , and  $U = 0.5\text{ m/s}$ . The figure shows that the double-shielded thermocouple behaves similarly to the single-shielded thermocouple, except that errors in the upper and lower layers are reduced further, and the region of rapidly increasing error in the lower layer is shifted to even higher  $T_\infty$ . This shift dramatically decreases the likelihood that extreme errors will occur in the lower layer, since the shift is toward

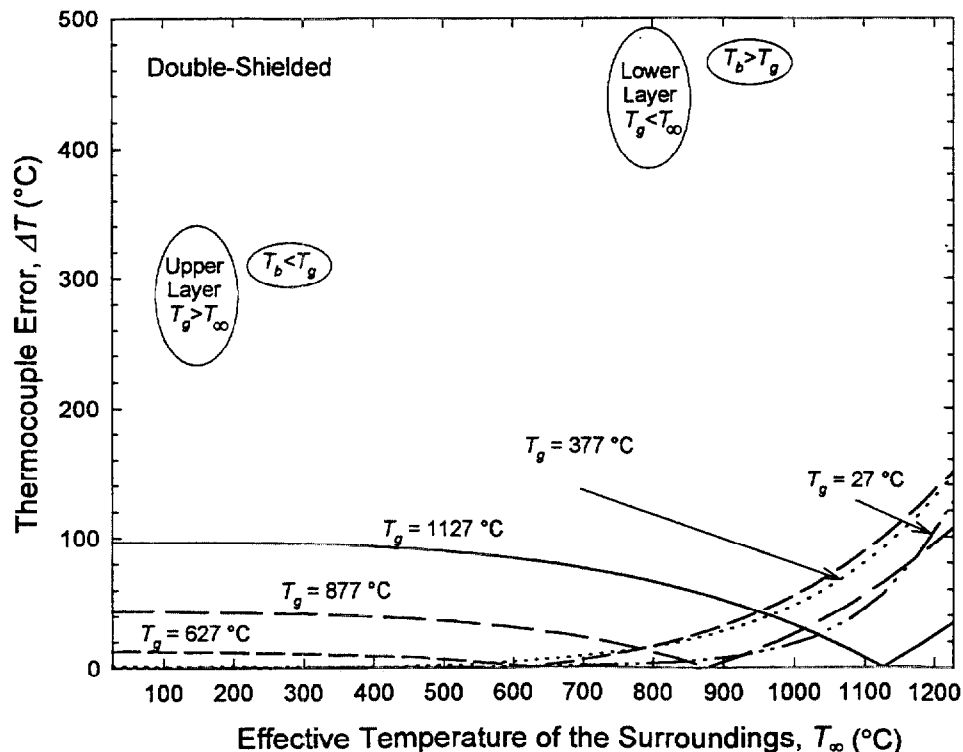


Fig. 6. Effect of surroundings temperature on absolute value of error in measured temperature (from Eq. (6)) for a double-shielded aspirated thermocouple, with bead diameter  $D_b = 1.5\text{ mm}$ , inner shield diameter  $D_i = 6.0\text{ mm}$ , outer shield diameter  $D_o = 8.6\text{ mm}$ , emissivities  $\varepsilon_b = \varepsilon_i = \varepsilon_o = 0.8$ , external velocity  $U = 0.5\text{ m/s}$ , and aspiration velocities  $u = 5\text{ m/s}$  and  $w = 5\text{ m/s}$ , and gas temperatures of  $27^\circ\text{C}$ ,  $377^\circ\text{C}$ ,  $627^\circ\text{C}$ ,  $877^\circ\text{C}$ , and  $1127^\circ\text{C}$ .

unrealistically high values of  $T_{\infty}$  for typical room fires. Subject to the present modeling assumptions, the upper-layer error for the double-shielded probe has an upper bound at 100°C for  $T_g = 1127^{\circ}\text{C}$ , which is about half of the 190°C bound of the single-shielded thermocouple exposed to the same conditions. Similar trends occur for the other conditions considered in the figure. Thus, the double-shielded probe represents a significant improvement over the single-shielded probe, both in the upper layer where steady-state errors are decreased to about half of their single-shield values, and in the lower layer where steady-state errors are reduced and the likelihood of occurrence of large errors is lessened. The improved performance of the double-shielded probe results from better radiation shielding and from higher convective heat transfer rates effected by the rapid flow through the annulus.

The results presented in this section reveal that lower-layer thermocouple errors are generally very sensitive to  $T_{\infty}$  for a given  $T_g$ . A small change in a fire can hence cause a very large change in the temperature indicated by a lower-layer thermocouple. Even aspirated thermocouples are susceptible to this radiation effect. It is worth mentioning that the  $T_{\infty}$  experienced by a thermocouple in any region of an enclosure fire generally increases as the fire grows. Hence, lower-layer thermocouple errors are likely to be low initially but increase in magnitude as time (and fire growth) progresses. Near flashover, room fire conditions change so rapidly that application of the present (or any other) model becomes extremely difficult.

One benefit of solving the types of equations developed here is that unusual data trends can be explained. For example, thermocouples used at floor level in the doorway of an enclosure should indicate ambient temperature since there is no preheat mechanism for the incoming air [29]. However, bare thermocouples used in these locations often indicate temperatures higher than room temperature [3–5,29]. Considering that lower-layer thermocouples are very susceptible to radiation errors of the type depicted on the right side of Fig. 4, this experimental result is not surprising.

It should be noted that the addition of each radiation shield increases the overall mass and volume of the thermocouple assembly. As a result, the ability of the probe to respond to fast fluctuations in  $T_g$  may be degraded relative to a bare thermocouple. Whether the error is improved or degraded depends on whether  $T_g$  is moving toward or away from the slower-responding inner shield temperature. These transient effects are not captured by the present steady-state modeling.

### 3.2. *Effect of aspiration velocity*

To demonstrate the role of aspiration velocity on the effectiveness of a single-shielded aspirated thermocouple, Figs. 7–9 depict its predicted response to changes in this velocity for selected upper- and lower-layer cases. A vertical line on each figure marks the 5-m/s aspiration velocity recommended for use with single-shielded thermocouples by ASTM. Horizontal lines on each figure mark the values of the gas and surroundings temperatures.

Fig. 7 shows predictions for selected upper- and lower-layer cases when the difference between  $T_g$  and  $T_{\infty}$  is 900°C. Results for an upper-layer case with  $T_g = 927^{\circ}\text{C}$  and  $T_{\infty} = 27^{\circ}\text{C}$  are shown along with predictions for a lower-layer case

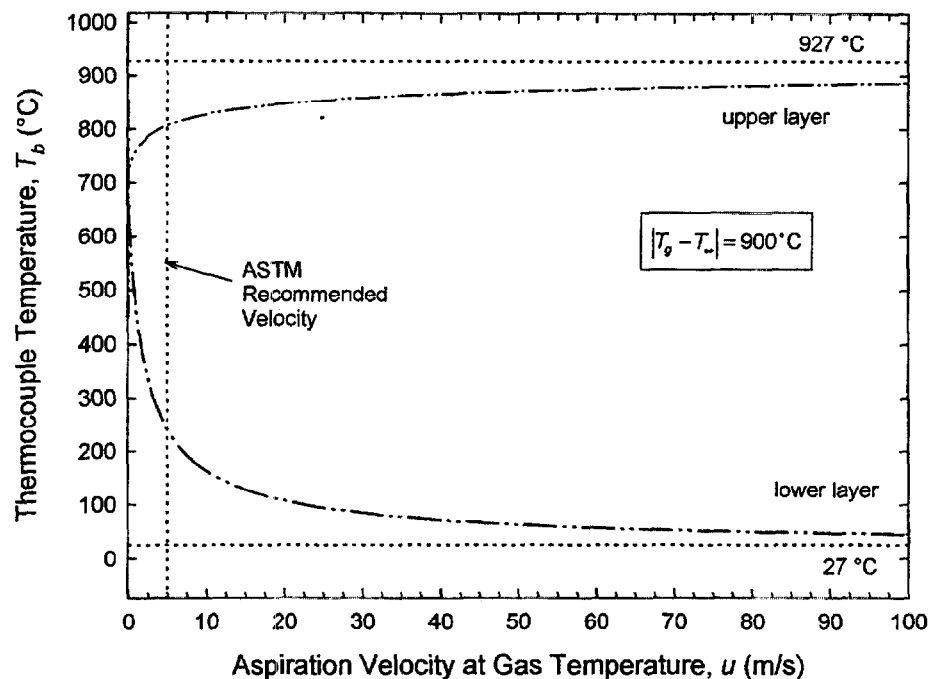


Fig. 7. Predicted single-shielded thermocouple response to variation in aspiration velocity for conditions with differences between  $T_g$  and  $T_\infty$  of  $900^\circ\text{C}$ . The upper-layer case corresponds to  $T_g = 927^\circ\text{C}$  and  $T_\infty = 27^\circ\text{C}$ , and the lower-layer case corresponds to  $T_g = 27^\circ\text{C}$  and  $T_\infty = 927^\circ\text{C}$ . The vertical line denotes the ASTM-recommended 5-m/s aspiration velocity, and horizontal lines mark the important temperatures of  $27^\circ\text{C}$  and  $927^\circ\text{C}$ .

with these values transposed ( $T_g = 27^\circ\text{C}$  and  $T_\infty = 927^\circ\text{C}$ ). These cases represent *extreme* but perhaps not impossible gas and surroundings temperature differences for a fire. As aspiration velocity is increased, the upper-layer thermocouple temperature increases suddenly from its no-aspiration value of  $450^\circ\text{C}$  to  $730^\circ\text{C}$ , and then rises gradually toward  $T_g$  ( $927^\circ\text{C}$ ). The lower-layer thermocouple temperature drops from its no-aspiration value of  $860^\circ\text{C}$  to  $690^\circ\text{C}$  and then gradually approaches  $T_g$  ( $27^\circ\text{C}$ ) as aspiration velocity is increased. Hence,  $T_b$  approaches  $T_g$  asymptotically as  $u$  is increased.

Fig. 8 shows predictions for selected upper- and lower-layer cases when the difference between  $T_g$  and  $T_\infty$  is  $600^\circ\text{C}$ . Results for an upper-layer case with  $T_g = 627^\circ\text{C}$  and  $T_\infty = 27^\circ\text{C}$  are shown along with predictions for a lower-layer case with  $T_g = 27^\circ\text{C}$  and  $T_\infty = 627^\circ\text{C}$ . These scenarios represent *moderate* gas and surroundings temperature differences which might occur during fire growth. As aspiration velocity is increased, the upper-layer thermocouple temperature increases suddenly from its no-aspiration value of  $360^\circ\text{C}$  to  $530^\circ\text{C}$ , and then rises gradually toward  $T_g$  ( $627^\circ\text{C}$ ). The lower-layer thermocouple temperature drops from its no-aspiration value of  $520^\circ\text{C}$  to  $270^\circ\text{C}$ , and subsequently approaches  $T_g$  ( $27^\circ\text{C}$ ). For the  $|T_g - T_\infty| = 600^\circ\text{C}$  curves shown in the figure,  $T_b$  approaches  $T_g$  more rapidly than for the  $|T_g - T_\infty| = 900^\circ\text{C}$  curves shown in Fig. 7.

Fig. 9 shows predictions for selected upper- and lower-layer cases when the difference between  $T_g$  and  $T_\infty$  is  $300^\circ\text{C}$ . Results for an upper layer case with



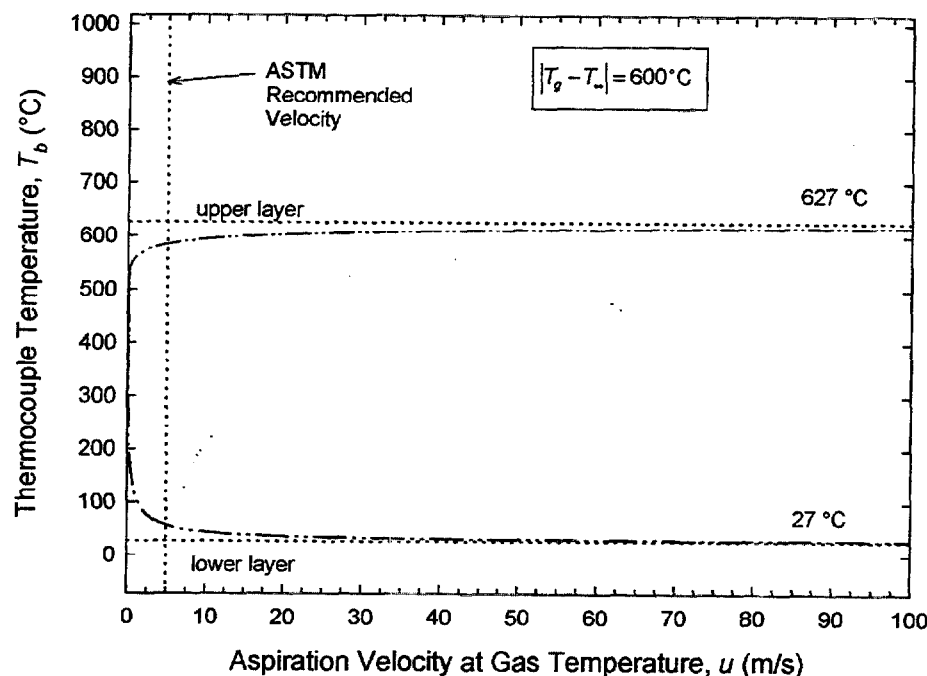


Fig. 8. Predicted single-shielded thermocouple response to variation in aspiration velocity for conditions with differences between  $T_g$  and  $T_\infty$  of 600°C. The upper-layer case corresponds to  $T_g = 627^\circ\text{C}$  and  $T_\infty = 27^\circ\text{C}$ , and the lower-layer case corresponds to  $T_g = 27^\circ\text{C}$  and  $T_\infty = 627^\circ\text{C}$ . The vertical line denotes the ASTM-recommended 5-m/s aspiration velocity, and horizontal lines mark the important temperatures of  $27^\circ\text{C}$  and  $627^\circ\text{C}$ .

$T_g = 327^\circ\text{C}$  and  $T_\infty = 27^\circ\text{C}$  are shown along with predictions for a lower layer case with  $T_g = 27^\circ\text{C}$  and  $T_\infty = 327^\circ\text{C}$ . These cases signify low gas and surroundings temperature differences which might occur during a room fire. As aspiration velocity is increased, the upper-layer thermocouple temperature increases suddenly from its no-aspiration value of  $290^\circ\text{C}$  to  $306^\circ\text{C}$ , and then rises immediately toward  $T_g$  ( $327^\circ\text{C}$ ). The lower-layer thermocouple temperature drops from its no-aspiration value of  $90^\circ\text{C}$  to  $50^\circ\text{C}$ , and rapidly approaches  $T_g$  ( $27^\circ\text{C}$ ). For the cases depicted in Fig. 9, the thermocouple temperature approximately equals  $T_g$  even for small values of aspiration velocity.

The results shown in Figs. 7–9 demonstrate that the temperature indicated by an aspirated thermocouple approaches the true gas temperature asymptotically as the velocity of the aspirating flow is increased. For low values of  $|T_g - T_\infty|$ , the thermocouple temperature approaches  $T_g$  more rapidly than for higher values of  $|T_g - T_\infty|$ . As the difference between  $T_g$  and  $T_\infty$  increases, larger and larger aspiration velocities are necessary to achieve a given accuracy level.

Table 1 summarizes the thermocouple errors derived from Figs. 7–9 for aspiration velocities of 5 m/s, 20 m/s, and 100 m/s. The percents error, defined in terms of absolute temperature as  $[\Delta T(K)/T_g(K)] \times 100\%$ , are shown in parentheses in the table. Once again, the numerical values of these errors apply only for the specific geometries and parameter choices described in this paper. The numbers are meant to provide order-of-magnitude information, and can be used to qualitatively judge when

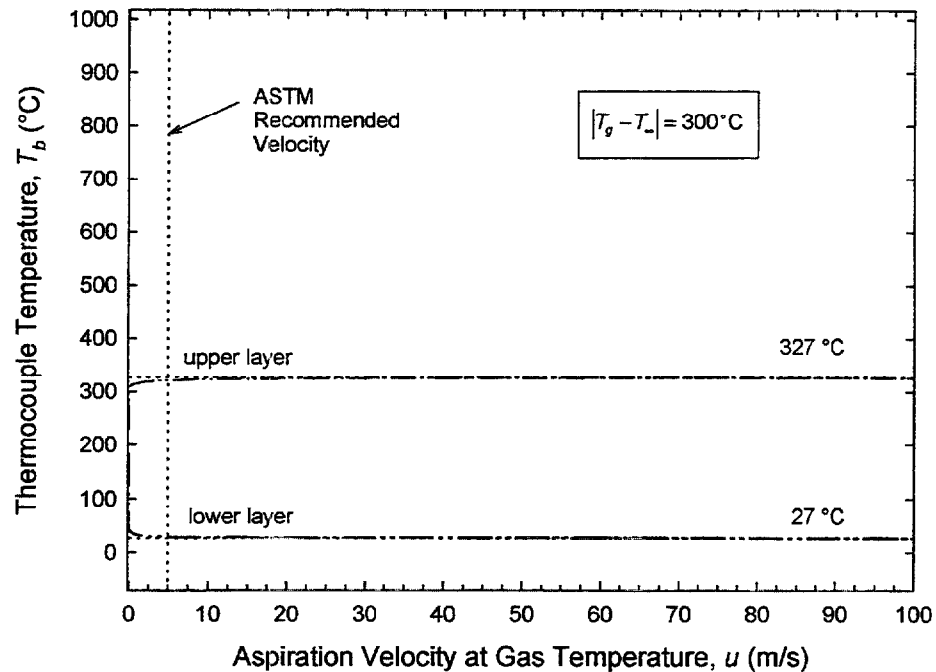


Fig. 9. Predicted single-shielded thermocouple response to variation in aspiration velocity for conditions with differences between  $T_g$  and  $T_\infty$  of  $300^\circ\text{C}$ . The upper-layer case corresponds to  $T_g = 327^\circ\text{C}$  and  $T_\infty = 27^\circ\text{C}$ , and the lower-layer case corresponds to  $T_g = 27^\circ\text{C}$  and  $T_\infty = 327^\circ\text{C}$ . The vertical line denotes the ASTM-recommended 5-m/s aspiration velocity, and horizontal lines mark the important temperatures of  $27^\circ\text{C}$  and  $327^\circ\text{C}$ .

errors are “small” and when they are “large”. For example, the error of  $\Delta T = 213^\circ\text{C}$  (or 71% of absolute gas temperature) for the lower-layer case with  $T_g = 27^\circ\text{C}$  and  $T_\infty = 927^\circ\text{C}$  is considered “large”. The results summarized in the table show that both “small” and “large” errors are possible when the ASTM-recommended 5 m/s aspiration velocity is used during the course of a fire test.

The determination of whether errors of a certain magnitude are acceptable is the responsibility of the individual researcher and will depend on his or her requirements. However, the results summarized in Table 1 show that the error of an aspirated thermocouple is extremely sensitive to the value of aspiration velocity. Clearly, the ASTM assertion that 5 m/s is “... sufficiently high to allow accurate temperature measurement based on thermocouple voltage alone, even within flame zones ...”, can be misleading when the difference between  $T_g$  and  $T_\infty$  is large, especially in a lower layer, even if the accuracy requirements are only moderate.

The predictions summarized in Table 1 verify that the practical combustor literature is correct in its assertion that the use of very high aspiration velocities (on the order of 100 m/s) reduces the error of an aspirated thermocouple. However, removing the large quantities of gas necessary to achieve aspiration velocities of 100 m/s is not, in general, practical for fire testing and research. Even if it were possible to produce such high aspiration velocities, Table 1 demonstrates that a thermocouple could still experience “large” errors for certain conditions (e.g.,  $\Delta T = 19^\circ\text{C}$  for  $T_g = 27^\circ\text{C}$  and

Table 1

Comparison of predicted thermocouple errors for upper- and lower-layer cases considered in Figs. 7–9. The numbers in parentheses indicate the values of  $[\Delta T(K)/T_g(K)] \times 100\%$ . The value of  $\Delta T$  in  $^{\circ}\text{C}$  is equivalent to the value of  $\Delta T$  in K, while  $T_g(K) = T_g(^{\circ}\text{C}) + 273$

Single-shielded aspirated thermocouple error, $\Delta T$			
	$u = 5 \text{ m/s}$	$u = 20 \text{ m/s}$	$u = 100 \text{ m/s}$
$T_g = 927^{\circ}\text{C}$			
$T_{\infty} = 27^{\circ}\text{C}$	117 $^{\circ}\text{C}$	79 $^{\circ}\text{C}$	40 $^{\circ}\text{C}$
Upper-layer	(9.8%)	(6.6%)	(3.3%)
$T_g = 27^{\circ}\text{C}$			
$T_{\infty} = 927^{\circ}\text{C}$	213 $^{\circ}\text{C}$	81 $^{\circ}\text{C}$	19 $^{\circ}\text{C}$
Lower-layer	(71%)	(27%)	(6.3%)
$T_g = 627^{\circ}\text{C}$			
$T_{\infty} = 27^{\circ}\text{C}$	42 $^{\circ}\text{C}$	24 $^{\circ}\text{C}$	10 $^{\circ}\text{C}$
Upper-layer	(4.7%)	(2.7%)	(1.1%)
$T_g = 27^{\circ}\text{C}$			
$T_{\infty} = 627^{\circ}\text{C}$	30 $^{\circ}\text{C}$	9 $^{\circ}\text{C}$	2 $^{\circ}\text{C}$
Lower-layer	(10%)	(3.0%)	(0.67%)
$T_g = 327^{\circ}\text{C}$			
$T_{\infty} = 27^{\circ}\text{C}$	6 $^{\circ}\text{C}$	3 $^{\circ}\text{C}$	1 $^{\circ}\text{C}$
Upper-layer	(1.0%)	(0.5%)	(0.17%)
$T_g = 27^{\circ}\text{C}$			
$T_{\infty} = 327^{\circ}\text{C}$	2 $^{\circ}\text{C}$	1 $^{\circ}\text{C}$	< 1 $^{\circ}\text{C}$
Lower-layer	(0.67%)	(0.34%)	(< 0.2%)

$T_{\infty} = 927^{\circ}\text{C}$ ). Hence, while aspirated thermocouples represent an improvement over bare thermocouples, they should be used with the understanding that they are susceptible to radiation error, especially when operated with low aspiration velocities [4]. This contradicts assertions made previously in the fire literature [3,24,25].

#### 4. Summary and conclusions

Heat-transfer models were developed for a bare thermocouple bead, for a single-shielded aspirated thermocouple probe, and for a double-shielded aspirated thermocouple probe. A parametric study was performed. While the absolute values of the errors presented here depend strongly on the configurations studied and the model assumptions, the relative trends between the different fire conditions and instruments allow general conclusions to be drawn.

First, both bare and aspirated thermocouples behave differently in an upper-layer of a room fire than in a lower layer. In an upper layer, for a given gas temperature, the

thermocouple error is relatively insensitive to surroundings temperature. In a lower layer, much larger errors which increase rapidly with surroundings temperature are possible. The most extreme errors occur in the lower layer when  $T_g$  is low and  $T_\infty$  is high.

Aspirated thermocouples reduce the magnitude of the errors in the upper and lower layers of a room fire and reduce the likelihood that large errors will occur in the lower layer by shifting the region of large error toward unrealistically high surroundings temperatures. Double-shielded aspirated designs perform better than single-shielded aspirated designs of similar outer diameter. The use of an aspirated thermocouple *reduces* the error, but does not *eliminate* it entirely; the ASTM assertion [25] that 5 m/s is “... sufficiently high to allow accurate temperature measurement based on thermocouple voltage alone, even within flame zones...”, can be misleading for certain fire conditions, even if accuracy requirements are only moderate.

The present study provides researchers with the tools necessary to develop steady-state engineering models of bare-bead and aspirated thermocouples, tailor them to their own needs, and use them side-by-side with experiments to assess potential measurement errors. The problem then becomes that of selecting values of  $T_\infty$ ,  $\epsilon$ , and  $U$  which describe the effective radiative and convective environments experienced by the thermocouple throughout the course of a fire. This proves to be a challenging task, because the conditions experienced vary with fire type, with location in a given fire, and with time at a given location. The models described here are presently being combined with experimental data collected at NIST to gain further insight into the difficult task of performing thermocouple uncertainty analyses in fire environments [5].

Finally, if the uncertainties in thermocouple measurements are to be confidently estimated for fires, future work must address the need to understand the transient radiative and convective environments experienced by each instrument. In the meantime, the type of simplified modeling presented here can provide a great deal of insight for researchers.

### Acknowledgements

The authors acknowledge Emil Braun, Marco Fernandez, Erik Johnsson, Richard Peacock, Paul Reneke, and the staff of the NIST large-scale test facility for performing experiments and for contributing to discussions which provided motivation for this modeling.

### References

- [1] Whitaker S. Forced convection heat transfer correlations for flow in pipes, past flat plates, single cylinders, single spheres, and for flow in packed beds and tube bundles. *A.I.Ch.E. J.* 1972;18:361–71.
- [2] Jones JC. On the use of metal sheathed thermocouples in a hot gas layer originating from a room fire. *J Fire Sci* 1995;13:257–60.
- [3] Luo M. Effects of radiation on temperature measurement in a fire environment. *J Fire Sci* 1997;15:443–61.
- [4] Pitts WM, Braun E, Peacock RD, Mitler HE, Johnsson EL, Reneke PA, Blevins LG. Temperature uncertainties for bare-bead and aspirated thermocouple measurements in fire environments. *Proceedings*

- of the Fourteenth Meeting of the U.S./Japan Government Cooperative Program on Natural Resources (UJNR) Panel on Fire Research and Safety, May 1998.
- [5] Pitts WM, Braun E, Peacock RD, Mitler HE, Johnsson EL, Reneke PA, Blevins LG. Thermocouple measurement in a fire environment. National Institute of Standards and Technology Internal Report Gaithersburg, Maryland, 1999, to appear.
- [6] Schack A. The theory and application of the suction pyrometer. *J Inst Fuel* 1939;12:S30–8.
- [7] Mulliken HF. Gas-temperature measurements and the high-velocity thermocouple. *Temperature: its measurement and control in science and industry*. New York: Reinhold, 1941. p. 775–804.
- [8] Mulliken HF, Osborn WJ. Accuracy tests of the high-velocity thermocouple. *Temperature: its measurement and control in science and industry*. New York: Reinhold, 1941. p. 805–829.
- [9] Barber R, Jackson R, Land T, Thurlow GG. A suction pyrometer for measuring gas exit temperatures from the combustion chambers of water-tube boilers. *J Inst Fuel* 1954;408–16.
- [10] Land T, Barber RB. The design of suction pyrometers. *Trans Soc Instr Technol* 1954;6:112–30.
- [11] Baker HD, Ryder EA, Baker NH. *Temperature measurements in engineering*, vol. II. New York: Wiley, 1961.
- [12] Hills AWD, Paulin A. The construction and calibration of an inexpensive microaspiration pyrometer. *J Sci Instr (J Phys E)* 1969;2:713–7.
- [13] Chedaille J, Braud Y. Industrial flames, vol I: measurements in flames. In: Beer JM, Thring MW, editors. New York: Crane, Russak, and Company, 1972.
- [14] Magidy PL, Lysakov II. Corrections of local values of flame temperature measured by suction pyrometers. *Heat Transfer—Sov Res* 1975;7:154–60.
- [15] Morillon R, Perthuis E. Pyrometres a aspiration: principes realisation d'instruments miniaturises. *Revue Generale de Thermique*. 1974;149:399–410.
- [16] Khalil MB, El-Mahallawy FM, Farag SA. Accuracy of temperature measurements in furnaces. *Lett Heat Mass Transfer* 1976;3:421–32.
- [17] Wojtan MS, Jones KAG. Improvements in the design and operation of a suction pyrometer. *Measure Control* 1981;14:301–5.
- [18] Goldman Y. Temperature measurement in combustors by use of suction pyrometry. *Combust Sci Technol* 1987;55:169–75.
- [19] Heitor MV, Moreira ALN. Thermocouples and sample probes for combustion studies. *Progr Energy Combust Sci* 1993;19:259–78.
- [20] Jones WP, Toral H. Temperature and composition measurements in a research gas turbine combustion chamber. *Combust Sci Technol* 1983;31:249–75.
- [21] Illerup J, Dam-Johansen K, Glarborg P. Characterization of a full-scale, single-burner pulverized coal boiler: temperatures, gas concentrations and nitrogen oxides. *Fuel* 1994;73:492–9.
- [22] Hughes PMJ, Lacelle RJ, Parameswaran T. A comparison of suction pyrometer and CARS derived temperatures in an industrial scale flame. *Combust Sci Technol* 1995;105:131–45.
- [23] Luckerath R, Woyde M, Meier W, Stricker W, Schnell U, Magel H, Gorres J, Hartmut S, Maier H. Comparison of coherent anti-stokes Raman-scattering thermometry with thermocouple measurements and model predictions in both natural-gas and coal-dust flames. *Appl Opt* 1995;34:3303–12.
- [24] Newman JS, Croce PA. A simple aspirated thermocouple for use in fire. *J Fire Flammability* 1979;10:327–36.
- [25] ASTM Standard E 603-98, 1998 Annual book of ASTM standards, vol. 04.07. West Conshohocken, Pennsylvania: American Society for Testing and Materials, 1998. p. 512.
- [26] Sparrow EM. On the calculation of radiant interchange between surfaces. In: Ibele WE, editor. *Modern developments in heat transfer*. New York: Academic Press, 1963. p. 181–212.
- [27] Modest MF. *Radiative heat transfer*. New York: McGraw-Hill, 1993.
- [28] Incropera FP, DeWitt DP. *Fundamentals of heat and mass transfer*, 3rd ed. New York: Wiley, 1990.
- [29] Steckler KD, Quintiere JG, Rinkinen WJ. Flow induced by fire in a compartment. National Bureau of Standards Internal Report NBSIR 82-2520, U.S. Department of Commerce, Gaithersburg, Maryland, 1982.
- [30] Omega temperature handbook. Omega Engineering Incorporated, 1996.